Chapter 1

The magnetocaloric effect

1.1 Introduction

The magnetocaloric effect (MCE) is defined as the heating or cooling (*i.e.*, the temperature change) of a magnetic material due to the application of a magnetic field. This effect has been called adiabatic demagnetisation for years, though this fenomenon is one practical application of the MCE in magnetic materials. For excellent reviews on the magnetocaloric effect, see references [1, 2].

The magnetocaloric effect was discovered in 1881, when Warburg observed it in iron [3]. The origin of the MCE was explained independently by Debye [4] and Giauque [5]. They also suggested the first practical use of the MCE: the adiabatic demagnetisation, used to reach temperatures lower than that of liquid helium, which had been the lowest achievable experimental temperature.

Nowadays, there is a great deal of interest in using the MCE as an alternative technology for refrigeration, from room temperature to the temperatures of hydrogen and helium liquefaction (~20-4.2 K). The magnetic refrigeration offers the prospect of an energy-efficient and environtment friendly alternative to the common vapour-cycle refrigeration technology in use today [6, 7].

1.2 Basic theory

In order to explain the origin of the magnetocaloric effect, we use thermodynamics, which relates the magnetic variables (magnetisation and magnetic field) to entropy and temperature. All magnetic materials intrinsically show MCE, although the intensity of the effect depends on the properties of each material. The physical origin of the MCE is the coupling of the magnetic sublattice to the applied magnetic field, H, which changes the magnetic contribution to the entropy of the solid. The equivalence to the thermodynamics of a gas is evident (see Fig.

1.1): the isothermal compression of a gas (we apply pressure and the entropy decreases) is analogous to the isothermal magnetisation of a paramagnet or a soft ferromagnet (we apply H and the magnetic entropy decreases), while the subsequent adiabatic expansion of a gas (we lower pressure at constant entropy and temperature decreases) is equivalent to adiabatic demagnetisation (we remove H, the total entropy remains constant and temperature decreases since the magnetic entropy increases).

The value of the entropy of a ferromagnet (FM) at constant pressure depends on both H and temperature, T, whose contributions are the lattice ($S_{\rm lat}$) and electronic ($S_{\rm el}$) entropies, as for any solid, and the magnetic entropy ($S_{\rm m}$),

$$S(T,H) = S_{\rm m}(T,H) + S_{\rm lat}(T) + S_{\rm el}(T) \ . \tag{1.1}$$

Figure 1.2 shows a diagram of the entropy of a FM near its Curie temperature, T_C, as a function of T. The total entropy is displayed for an applied external field, H_1, and for zero field, H_0. The magnetic part of the entropy is also shown for each case (H_1 and H_0).

Two relevant processes are shown in the diagram in order to understand the thermodynamics of the MCE:

(i) When the magnetic field is applied adiabatically (*i.e.*, the total entropy remains constant) in a reversible process, the magnetic entropy decreases, but as the total entropy does not change, *i.e.*,

$$S(T_0,H_0) = S(T_1,H_1) \ , \tag{1.2}$$

then, the temperature increases. This adiabatic temperature rise can be visualised as the isentropic difference between the corresponding $S(T,H)$ functions and it is a measurement of the MCE in the material,

$$\Delta T_{ad} = T_1 - T_0 \ . \tag{1.3}$$

(ii) When the magnetic field is applied isothermally (T remains constant), the total entropy decreases due to the decrease in the magnetic contribution, and therefore the entropy change in the process is defined as

$$\Delta S_m = S(T_0,H_0) - S(T_0,H_1) \ . \tag{1.4}$$

Both the adiabatic temperature change, ΔT_{ad}, and the isothermal magnetic entropy change, ΔS_m, are characteristic values of the MCE. Both quantities are functions of the initial temperature, T_0, and the magnetic field variation $\Delta H = H_1 - H_0$.

Therefore, it is straightforward to see that if rising the field increases magnetic order (*i.e.*, decreases magnetic entropy), then $\Delta T_{ad}(T,\Delta H)$ is positive and magnetic solid heats up, while $\Delta S_m(T,\Delta H)$ is negative. But if the field is reduced,

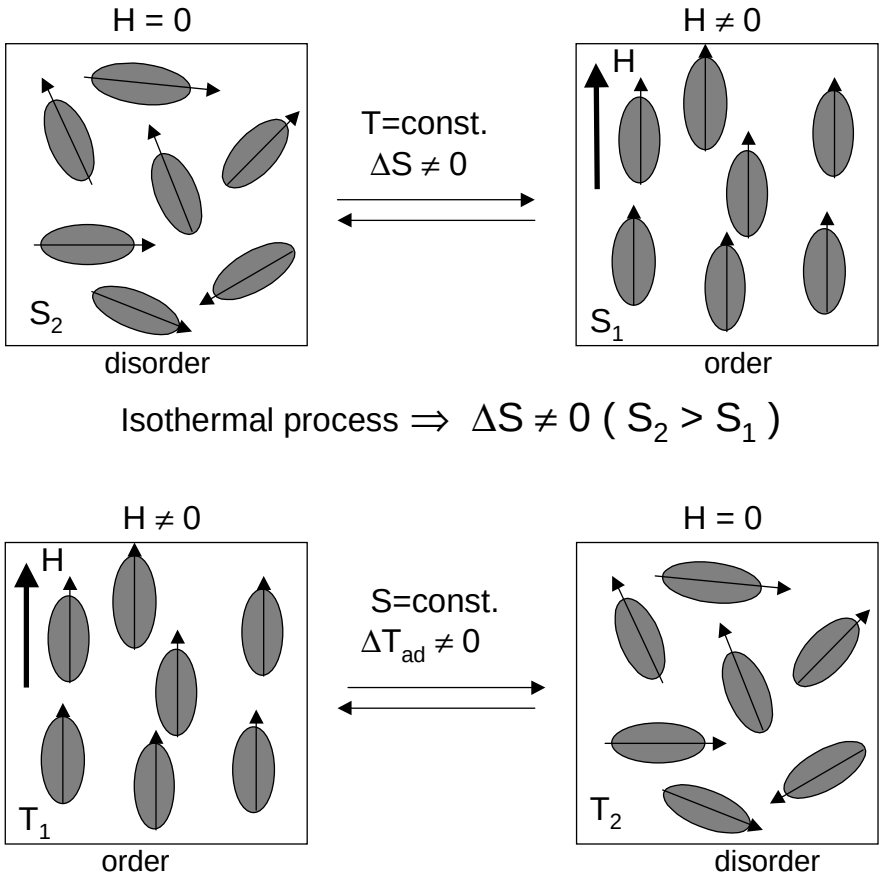

Figure 1.1: Schematic picture that shows the two basic processes of the magnetocaloric effect when a magnetic field is applied or removed in a magnetic system: the isothermal process, which leads to an entropy change, and the adiabatic process, which yields a variation in temperature.

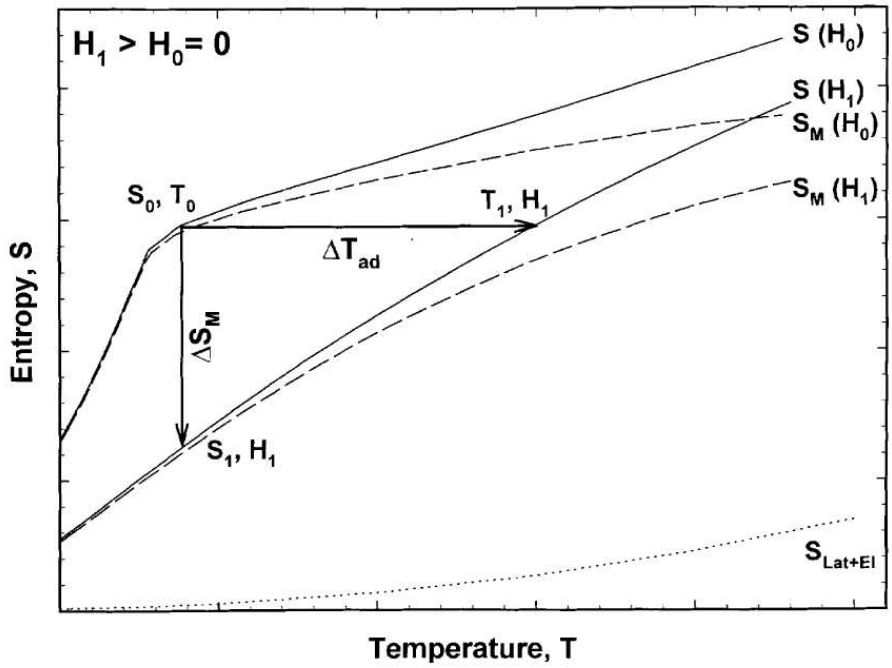

Figure 1.2: $S - T$ diagram showing the MCE. Solid lines represent the total entropy in two different magnetic fields ($H_0 = 0$ and $H_1 > 0$), dotted line shows the electronic and lattice contributions to the entropy (non-magnetic), and dashed lines show the magnetic entropy in the two fields. The horizontal arrow shows ΔT_{ad} and the vertical arrow shows ΔS_m, when the magnetic field is changed from H_0 to H_1. Taken from Ref. [2].

magnetic order decreases and $\Delta T_{ad}(T, -\Delta H)$ is thus negative, while $\Delta S_m(T, -\Delta H)$ is positive, giving rise to a cooling of the magnetic solid.

The relation between H, the magnetisation of the material, M, and T, to the MCE values, $\Delta T_{ad}(T, \Delta H)$ and $\Delta S_m(T, \Delta H)$, is given by one of the Maxwell relations [8],

$$\left(\frac{\partial S(T,H)}{\partial H}\right)_T = \left(\frac{\partial M(T,H)}{\partial T}\right)_H \quad . \tag{1.5}$$

Integrating Eq. 1.5 for an isothermal (and isobaric) process, we obtain

$$\Delta S_m(T, \Delta H) = \int_{H_1}^{H_2} \left(\frac{\partial M(T,H)}{\partial T}\right)_H dH \quad . \tag{1.6}$$

This equation indicates that the magnetic entropy change is proportional to both the derivative of magnetisation with respect to temperature at constant field and to the field variation. Using the following thermodynamic relations [8]:

$$\left(\frac{\partial T}{\partial H}\right)_S = -\left(\frac{\partial S}{\partial H}\right)_T \left(\frac{\partial T}{\partial S}\right)_H \tag{1.7}$$

$$C_H = T\left(\frac{\partial S}{\partial T}\right)_H \quad , \tag{1.8}$$

where C_H is the heat capacity at constant field, and taking into account Eq. 1.5, the infinitesimal adiabatic temperature change is given by

$$dT)_{ad} = -\left(\frac{T}{C(T,H)}\right)_H \left(\frac{\partial M(T,H)}{\partial T}\right)_H dH \quad . \tag{1.9}$$

After integrating this equation, we obtain other expresion that characterises the magnetocaloric effect,

$$\Delta T_{ad}(T, \Delta H) = -\int_{H_1}^{H_2} \left(\frac{T}{C(T,H)}\right)_H \left(\frac{\partial M(T,H)}{\partial T}\right)_H dH \quad . \tag{1.10}$$

By analysing Eqs. 1.6 and 1.10, some information about the behaviour of the MCE in solids can be gained:

1. Magnetisation at constant field in both paramagnets (PM) and simple FMs decreases with increasing temperature, *i.e.*, $(\partial M/\partial T)_H < 0$. Hence $\Delta T_{ad}(T, \Delta H)$ should be positive, while $\Delta S_m(T, \Delta H)$ should be negative for positive field changes, $\Delta H > 0$.

2. In FMs, the absolute value of the derivative of magnetisation with respect to temperature, $|(\partial M/\partial T)_H|$, is maximum at T_C, and therefore $|\Delta S_m(T, \Delta H)|$ should show peak at $T = T_C$.

3. Although it is not straightforward from Eq. 1.10 since the heat capacity at constant field shows an anomalous behaviour near T_C, $\Delta T_{ad}(T, \Delta H)$ in FMs shows a peak at the Curie temperature when ΔH tends to zero [9].

4. For the same $|\Delta S_m(T, \Delta H)|$ value, the $\Delta T_{ad}(T, \Delta H)$ value will be larger at higher T and lower heat capacity.

5. In PMs, the $\Delta T_{ad}(T, \Delta H)$ value is only significant at temperatures close to absolute zero, since $|(\partial M/\partial T)_H|$ is otherwise small. Only when the heat capacity is also very small (same order as $|(\partial M/\partial T)_H|$), can a relevant $\Delta T_{ad}(T, \Delta H)$ value be obtained, which also happens only close to absolute zero. If we are interested in sizeable $\Delta T_{ad}(T, \Delta H)$ values at higher temperatures, we thus need a solid that orders spontaneously.

1.3 Mesurement of the magnetocaloric effect

1.3.1 Direct measurements

Direct techniques to measure MCE always involve the measurement of the initial (T_0) and final (T_F) temperatures of the sample, when the external magnetic field is changed from an initial (H_0) to a final value (H_F). Then the measurement of the adiabatic temperature change is simply given by

$$\Delta T_{ad}(T_0, H_F - H_0) = T_F - T_0 \ . \tag{1.11}$$

Direct measurement techniques can be performed using contact and non-contact techniques, depending on whether the temperature sensor is directly connected to the sample or not.

To perform direct measurements of MCE, a rapid change of the magnetic field is needed. Therefore, the measurements can be carried out either on immobilised samples by changing the field [10] or by moving the sample in and out of a constant magnetic field region [11]. Using immobilised samples and pulsed magnetic fields, direct MCE measurements from 1 to 40 Tesla (T) have been reported. When electromagnets are used, the magnetic field is usually reduced to less than 2 T. When the sample or the magnet are moved, permanent or superconducting magnets are usually employed, with a magnetic field range of 0.1-10 T.

The accuracy of the direct experimental techniques depends on the errors in thermometry and in field setting, the quality of thermal insulation of the sample, the possible modification of the reading of temperature sensor due to the applied field, etc. Considering all these effects, the accuracy is claimed to be within the 5-10% range [2, 10, 11].

At this point, we must mention the new direct measurement of MCE associated with first-order field-induced magnetic phase transitions, that is presented in this

thesis (see Chapter 4): a differential scanning calorimeter (DSC) operating under applied magnetic field that measures the enthalpy of transformation (*i.e.*, the latent heat) when the transition is induced by field. From the latent heat, the entropy change is obtained, being the first direct measurement of MCE performed through the entropy change.

1.3.2 Indirect measurements

Unlike direct measurements, which usually only yield the adiabatic temperature change, indirect experiments allow the calculation of both $\Delta T_{ad}(T, \Delta H)$ and $\Delta S_m(T, \Delta H)$ in the case of heat capacity measurements, or just $\Delta S_m(T, \Delta H)$ in the case of magnetisation measurements. In the latter case, magnetisation must be measured as a function of T and H. This allows to obtain $\Delta S_m(T, \Delta H)$ by numerical integration of Eq. 1.6, and it is very useful as a rapid search for potential magnetic refrigerant materials [12]. The accuracy of $\Delta S_m(T, \Delta H)$ calculated from magnetisation data depends on the accuracy of the measurements of the magnetic moment, T and H. It is also affected by the fact that the exact differentials in Eq. 1.6 (dM, dH and dT) are replaced by the measured variations (ΔM, ΔT and ΔH). Taking into account all these effects, the error in the value of $\Delta S_m(T, \Delta H)$ lies within the range of 3-10% [2, 12].

The measurement of the heat capacity as a funcion of temperature in constant magnetic fields and pressure, $C(T)_{P,H}$, provides the most complete characterisation of MCE in magnetic materials. The entropy of a solid can be calculated from the heat capacity as:

$$S(T)_{H=0} = \int_0^T \frac{C(T)_{P,H=0}}{T}\, dT + S_0$$
$$S(T)_{H\neq 0} = \int_0^T \frac{C(T)_{P,H}}{T}\, dT + S_{0,H} \quad , \tag{1.12}$$

where S_0 and $S_{0,H}$ are the zero temperature entropies. In a condensed system $S_0 = S_{0,H}$ [14]. Hence, if $S(T)_H$ is known, both $\Delta T_{ad}(T, \Delta H)$ and $\Delta S_m(T, \Delta H)$ can be obtained [15], see for example Fig. 1.3. However, this evaluation is not valid if a first-order transition takes place within the evaluated range, since the value of C_P is not defined at a first order transition (see Refs. [16, 17] and Chapter 4). In this case, the entropy curves present a discontinuity, which corresponds to the entropy change of the transition. The entropy discontinuity can be determined from different experimental data, such as magnetisation or DSC, and then the resulting $S(T)_H$ functions can be corrected accordingly [16].

The accuracy in the measurements of MCE using heat capacity data depends critically on the accuracy of $C(T)_{P,H}$ measurements and data processing, since

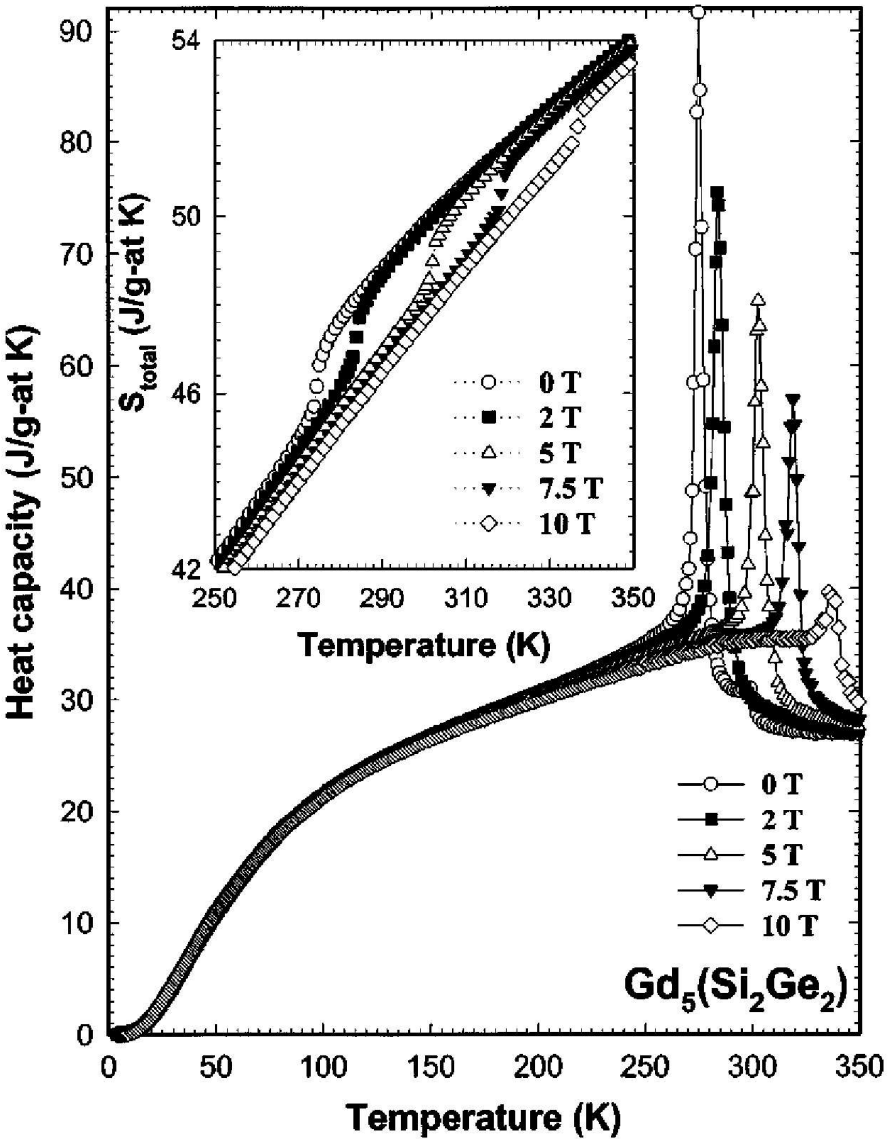

Figure 1.3: Heat capacity of $Gd_5(Si_2Ge_2)$ as a function of temperature under different applied fields. The inset displays the total entropy as a function of temperature at different fields, as determined from heat capacity. From these curves, ΔS_m and ΔT_{ad} are easily obtained. Taken from Ref. [13].

both $\Delta T_{ad}(T, \Delta H)$ and $\Delta S_m(T, \Delta H)$ are small differences between two large values (temperatures and total entropies). The error in $\Delta S_m(T, \Delta H)$, $\sigma[\Delta S_m(T, \Delta H)]$, calculated from heat capacity is given by the expression [15]

$$\sigma[\Delta S_m(T, \Delta H)] = \sigma[S(T, H = 0)] + \sigma[S(T, H \neq 0)] \ , \qquad (1.13)$$

where $\sigma S(T, H = 0)$ and $\sigma S(T, H \neq 0)$ are the errors in the calculation of the zero field entropy and non-zero field entropy, respectively. The error in the value of the adiabatic temperature change, $\sigma[\Delta T_{ad}(T, \Delta H)]$, is also proportional to the errors in the entropy, but it is inversely proportional to the derivative of the entropy with respect to temperature [15]:

$$\sigma[\Delta T_{ad}(T, \Delta H)] = \frac{\sigma[S(T, H = 0)]}{\left(\frac{dS(T,H=0)}{dT}\right)} + \frac{\sigma[S(T, H \neq 0)]}{\left(\frac{dS(T,H\neq 0)}{dT}\right)} \ . \qquad (1.14)$$

It is worth noting that Eqs. 1.13 and 1.14 yield the absolute error in MCE measurements and, therefore, the relative errors strongly increase for small MCE values (see Fig. 1.4). Assuming thus that the accuracy of the heat capacity measurements is not field dependent, the relative error in both $\Delta T_{ad}(T, \Delta H)$ and $\Delta S_m(T, \Delta H)$ is reduced for larger ΔH values.

1.4 Magnetocaloric effect in paramagnets

MCE in PMs was used as the first practical application, the so-called adiabatic demagnetisation. With this technique, ultra-low temperatures can be reached (mK-μK). In 1927, the pioneering work of Giauque and MacDougall [5, 18] showed that using the paramagnetic salt $Gd_2(SO_4)_3 \cdot 8H_2O$, T lower than 1 K could be reached. Later, MCE at low temperatures was studied in other PM salts, such as ferric ammonium alum $[Fe(NH_4)(SO_4) \cdot 2H_2O]$ [19], chromic potassium alum [20] and cerous magnesium nitrate [21]. The problem for the practical application of adiabatic demagnetisation using PM salts lies in its low thermal conductivity. Hence, the next step was the study of PM intermetallic compounds. One of the most studied materials was $PrNi_5$ and it is actually still used in nuclear adiabatic demagnetisation devices. Using $PrNi_5$ the lowest working temperature has been reached: 27 μK [22]. Another group of materials that have extensively been studied are PM garnets, because of their high thermal conductivity, low lattice heat capacity and very low ordering temperature (usually below 1 K). An ordering temperature so close to absolute zero allows to obtain a large ΔS_m and to keep a significant MCE up to ~20K. For instance, ΔT_{ad} within 6 and 10 K have been reached in ytterbium ($Y_3Fe_5O_{12}$) and gadolinium ($Gd_3Fe_5O_{12}$) iron garnets, with $\mu_0 \Delta H$ = 11 T, in the 10-30 K T-range [23]. Appreciable MCE values have also

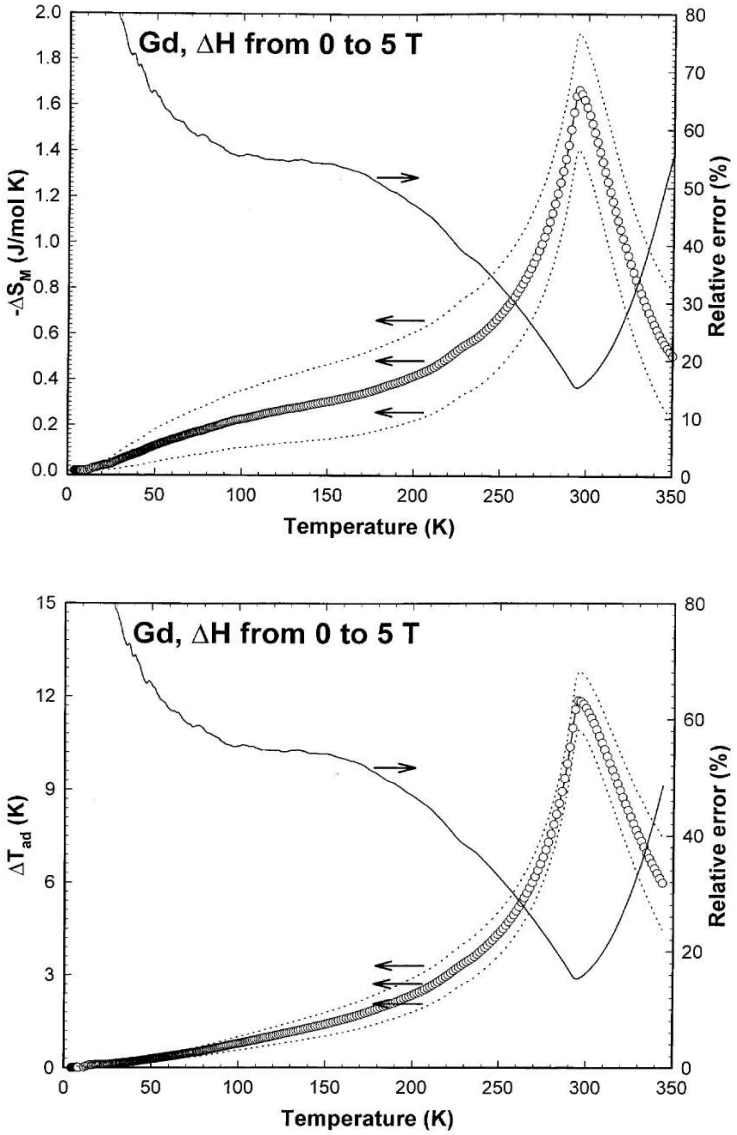

Figure 1.4: ΔS_m and ΔT_{ad} values in Gd for a magnetic field change from 0 to 5 T and calculated from the experimental heat capacity data measured at 0 and 5 T (open circles). The dotted lines indicate the range of absolute errors and the solid lines show the relative error of the calculated values. Taken from Ref. [2].

been reached using neodymium gallium garnet ($Nd_3Ga_5O_{12}$) at 4.2 K [24] and gadolinium gallium garnet ($Gd_3Ga_5O_{12}$) below 15 K [25]. Finally, a large value of ΔS_m has been observed in magnetic nanocomposites based on the iron-substituted gadolinium gallium garnets, $Gd_3Ga_{5-x}Fe_xO_{12}$, for $x \leq 2.5$ [26].

1.5 MCE in order-disorder magnetic phase transitions

Spontaneous magnetic ordering of PM solids below a given temperature is a cooperative phenomenon. The ordering temperature depends on the strenght of exchange interaction and on the nature of the magnetic sublattice in the material. When spontaneous magnetic ordering occurs, the magnetisation strongly varies in a very narrow temperature range in the vicinity of the transition temperature, *i.e.*, the Néel temperature for antiferromagnets (AFMs) and the Curie temperature for FMs. The fact that $|(\partial M/\partial T)_H|$ is large allows these magnetic materials to have a significant MCE. Since it is not the absolute value of the magnetisation, but rather its derivative with respect to temperature the one that must be large to obtain a large MCE, rare-earth metals or lanthanides (4f metals) and their alloys have been studied much more extensively than 3d transition metals and their alloys, because the available magnetic entropy in rare earths is considerably larger than in 3d transition metals: the maximum magnetic entropy for a lanthanide is $S_m = R\,ln(2J+1)$, where R is the universal gas constant and J is the total angular momentum.

The MCE in the vicinity of an order-disorder magnetic phase transition is calculated by using equations 1.6 and 1.10, which arise from the Maxwell relation (Eq. 1.5), since these transitions are second-order and thermodynamic variables change continuously [1, 17]. The research on these type of materials has been centered in soft FMs with T_C between 4 and 77 K, suitable for applications such as for example helium and nitrogen liquefaction, and also in materials which order near room temperature so as to use their magnetocaloric properties in magnetic refrigeration and air conditioning.

1.5.1 MCE in the low-temperature range (~10-80 K)

The first evident choise for low-temperature magnetic refrigerant materials are some pure rare earths such as Nd, Er and Tm, since they order at low temperatures. Anyway, the expectations for large MCE are not fulfilled. MCE in Nd reach $\Delta T_{ad} \sim 2.5$ K at T=10 K for a magnetic field rise $\mu_0\Delta H = 10$ T [27]. The problem in Er is that several magnetic phase transitions occur between 20 and 80 K,

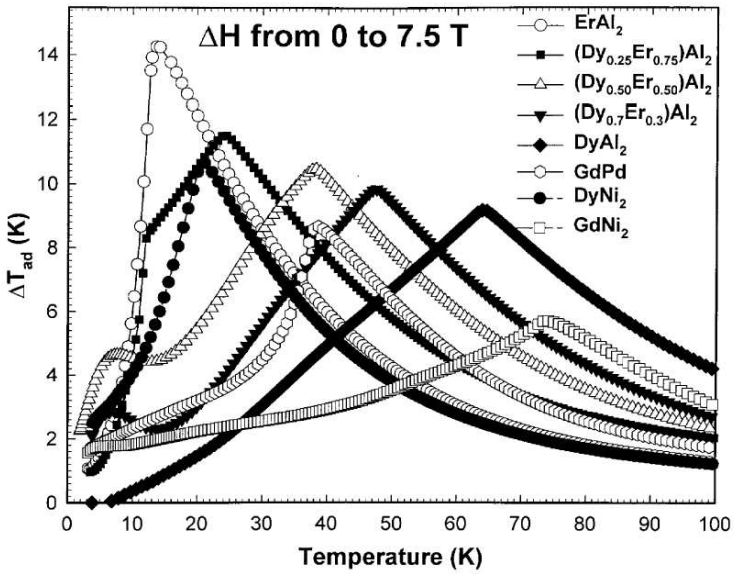

Figure 1.5: The adiabatic temperature change in the best magnetic refrigerant intermetallic materials in the temperature range from~10 K to ~80 K, for a magnetic field change between 0 and 7.5 T. Taken from Ref. [2].

which causes the MCE to be constant but small in this overall temperature range: $\Delta T_{ad} \sim 4-5$ K for $\mu_0 \Delta H = 7$ T [28]. Tm has a peculiar magnetic behaviour: it orders magnetically in a sinusoidally modulated ferromagnetic structure at~56 K and becomes ferrimagnetic at ~32 K. These features bring about both a restricted MCE, which barely reaches $\Delta T_{ad} \sim 3$ K at T =56 K for $\mu_0 \Delta H = 7$ T, and a negative ΔT_{ad} between 32 and 56 K for $\mu_0 \Delta H = 1$ T [29]. Consequently, the reason why MCE in these pure materials is so small is that most of magnetic phases in Nd, Er and Tm are either antiferromagnetic or ferrimagnetic, so that much of the available entropy is used in flipping spins to a ferromagnetic order.

The materials which display the largest MCE in the~10-80 K range are intermetallic compounds which contain lanthanide metals. The best of them are $REAl_2$ compounds, where RE = Er, Ho, Dy, $Dy_{0.5}Ho_{0.5}$ [30] and Dy_xEr_{1-x} ($0 \leq x \leq 1$) [9, 31], GdPd [9, 32], and $RENi_2$, where RE=Gd [33], Dy [34] and Ho[34]. Adiabatic temperature changes for some of them are shown in Fig. 1.5. The maximum MCE peak is reduced as temperature increases from 10 to 80 K, which is associated with the rapid rise of the lattice heat capacity with temperature in these alloys. The field dependence of the MCE in this temperature range varies within ~1 and ~2 K/T.

1.5.2 MCE in the intermediate-temperature range (~80-250 K)

This temperature range has not been much studied, mainly for two reasons. First, there are not many applications in this range (it lies above gas liquefactions and below room temperature). Second, the T/C fraction (where C is the phononic and electronic contribution to heat capacity) presents an inherent minimum in metals, as shown in figure 1.6 for a typical metal (Cu). This suggests that the adiabatic temperature variation is minimal in this temperature range (see equations 1.9 and 1.10).

One of the best magnetic refrigerant materials in this temperature range is pure Dy [9, 35], with $\Delta T_{ad} \sim 12$ K at $T \sim 180$ K for a magnetic field change $\mu_0 \Delta H = 7$ T. As discussed earlier for Tm (section 1.5.1), Dy also presents complex magnetic structures, which brings about a negative MCE for small field changes ($\mu_0 \Delta H < 2$ T). Recent works [36, 37] have also found a noticeable MCE in amorphous $RE_x(T_1,T_2)_{1-x}$ alloys, where RE is a rare earth metal and T_1, T_2 are $3d$ transition metals, in the range 100-200 K. The field dependence of the MCE is 2 K/T for Dy, but for the rest of the materials, such as those amorphous alloys, rarely reaches 1 K/T. In spite of all these difficulties for the MCE at the intermediate temperatures, the recently discovered $Gd_5(Si_xGe_{1-x})_4$ alloys show extremely large ΔS_m and ΔT_{ad} values, from 2 to 10 times larger than any of the above mentioned materials [38, 39]. We will later discuss on these alloys, since they are also foreseen as excellent magnetic refigerant materials at room temperature (see section 1.5.3). The origin of this giant MCE is explained in section 1.6, while their properties are exhaustively discussed in chapter 2.

1.5.3 MCE near room temperature

The prototype material at room temperature is Gd, a rare earth metal which orders FM at T_C=294 K. This lanthanide has been extensively studied [9, 10, 40, 41], and ΔT_{ad} values at T_C are ~6, 12, 16 and 20 K for magnetic field changes $\mu_0 \Delta H = 2$, 5, 7.5 and 10 T, respetively, leading to a field dependence of the MCE of ~3 K/T at low fields, which reduces to ~2 K/T at higher fields. A variety of alloys using Gd and other rare earths have been prepared in order to improve the MCE in Gd. Gd-RE alloys, with RE=lanthanide (Tb, Dy, Er, Ho,...) [42, 43] and/or Y [44] have been studied, but the alloying only decreases T_C - which is not desirable, since we depart from room temperature - while the MCE value does not increase considerably with respect to pure Gd. The only exceptions are nanocrystalline Gd-Y alloys, which improve the MCE in Gd for $\mu_0 \Delta H = 1$ T [45]. Most intermetallic compounds that order magnetically near room temperature and above ~290 K show a noticeble lower MCE than that of Gd. For example Y_2Fe_{17}, with $T_C \sim 310$ K, yields a MCE which is about 50% of that in Gd [46]. The same magnitude is

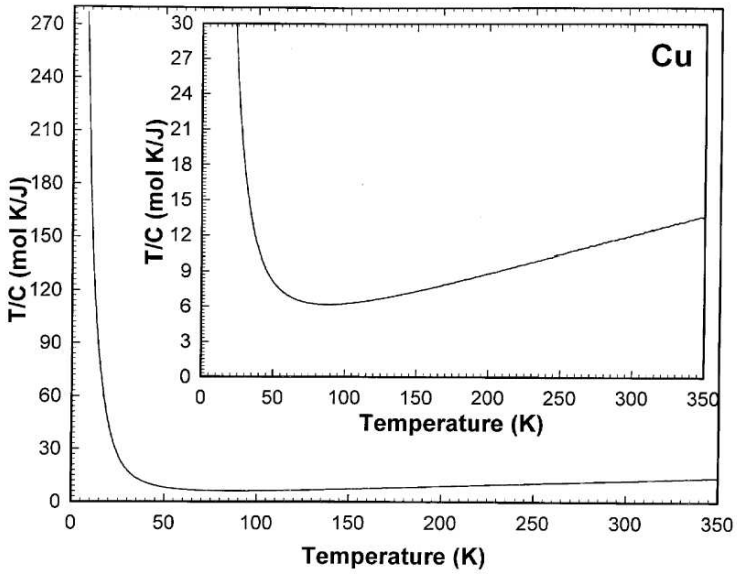

Figure 1.6: T/C versus T, where C is the electronic and phononic contribution of heat capacity in a typical metal (Cu). Taken from Ref. [2].

approximately measured in Nd_2Fe_{17} [46], with T_C ~324 K. It has been suggested that $(Pr_{1.5}Ce_{0.5})Fe_{17}$ could have a MCE larger than that of Gd, but it has not been verified experimentally [47]. The only intermetallic compounds that display a MCE as large as that of Gd are Gd_5Si_4 (with T_C ~335 K) and the germanium-substituted solid solution $Gd_5(Si_xGe_{1-x})_4$, for $0.5 \leq x \leq 1$, with T_C from ~290 to ~335 K [38]. In chapter 2, the main features of these alloys will be discussed in detail.

1.6 MCE in first-order magnetic phase transitions and the giant effect

In second-order magnetic phase transitions, the existence of short-range order and spin fluctuations above the order temperature (T_C) brings about a reduction in the maximum possible $|(\partial M/\partial T)_H|$ value, and the maximum MCE is accordingly reduced. In contrast, a first-order phase transition ideally occurs at constant temperature (the transition temperature, T_t) and thus the $|(\partial M/\partial T)_H|$ value should be infinitely large. Actually, in an ideal first-order phase transition, the discontinuity in both magnetisation and entropy causes that the derivatives in the mostly used Maxwell relation (equations 1.5 and 1.6) must be replaced by the finite increments

of the Clausius-Clapeyron equation for phase transformations. The discontinuity in the entropy is related to the entalphy of transformation, which is also called latent heat. The first-order transition occurs if the two magnetic phases have equal thermodynamic potential [48, 49],

$$\left[U_1 - \frac{n_1 M_1^2}{2}\right] - \Theta S_1 + (pV_1 - HM_1) = \left[U_2 - \frac{n_2 M_2^2}{2}\right] - \Theta S_2 + (pV_2 - HM_2) \ , \quad (1.15)$$

where Θ is the transition temperature at the field H, and $U_{1,2}$, $S_{1,2}$, $V_{1,2}$, $M_{1,2}$ are the internal energy, entropy, volume and magnetisation of phases 1 and 2, and nM^2 describes the molecular field contribution. If we assume that the external field only triggers the transition, but does not change the value of the physical parameters (S, M, V, n) in either phase, the difference of the transition temperature for a field change of ΔH is given as

$$\frac{\Delta\Theta}{\Delta H} = -\frac{\Delta M}{\Delta S} = \text{const} \ , \quad (1.16)$$

where $\Delta M = M_2 - M_1$ is the difference between the magnetisations and $\Delta S = S_2 - S_1$ the difference between the entropies of the two phases. The sign appears since a magnetised phase has lower entropy. $\Delta\Theta/\Delta H$ is the shift of the transition temperature with the transition field, which is usually evaluated as dT_t/dH_t from a $T_t(H_t)$ curve. Therefore, the Clausius-Clapyron equation is written as

$$\Delta S = -\Delta M \frac{dH_t}{dT_t} \ . \quad (1.17)$$

Chapter 5 discusses extensively the use of the Clausius-Clapeyron equation. The existence of this entropy change associated with the first-order transition brings about an extra contribution to MCE, yielding the so-called giant magnetocaloric effect. The use of this entropy change can be possible provided that the phase transition -and thus the entropy change- is induced by magnetic field. Extensively search for materials with a first-order field-induced magnetic phase transition has lately been shown in literature.

The intermetallic compound FeRh was one of the first materials in which this type of giant (and negative) MCE was observed. This alloy has a first-order FM-to-AFM phase transition at $T_t \sim 316$ K, which yields a MCE value as large as -8.4 K for $\mu_0\Delta H = 2.1$ T [50]. Unfortunately the giant effect is irreversible, and giant MCE can only be observed in virgin samples.

The recently discovered $Gd_5(Si_xGe_{1-x})_4$ alloys with $0 \leq x \leq 0.5$, display a ΔS_m at least twice larger than that of Gd near room temperature (-18.5 J/(kgK) for $\mu_0\Delta H = 5$ T at $T = 276$ K) [13], and between 2 and 10 times larger than the best magnetocaloric materials in the low and intermediate temperature ranges (-26 J/(kgK) at $T \sim 40$ K to -68 J/(kgK) at $T \sim 145$ K for $\mu_0\Delta H = 5$ T, depending

on composition, x) [38]. ΔT_{ad} is also very large, reaching for example 15.2 K for $\mu_0\Delta H$ = 5 T at T= 276 K and 15 K for $\mu_0\Delta H$ = 5 T at T ~ 70 K [39]. These alloys have some interesting properties that make them very exciting and candidates to be used as magnetic refrigerant materials in highly efficient magnetic refrigerators. The first one is that the transition temperature can be tuned from ~20 K to ~276 K by just changing the ratio between Si and Ge contents ($0 \leq x \leq 0.5$) [38, 51], and even a T_t ~305 K can be achieved by adding Ga impurities to $Gd_5(Si_2Ge_2)$ [52]. This allows one to shift at own's will the maximum giant MCE between ~20 and ~305 K. The second property is that, unlike FeRh, $Gd_5(Si_xGe_{1-x})_4$ alloys show a reversible MCE, *i.e.*, MCE does not disappear after the first application of a magnetic field. The difference in the behaviour of FeRh and $Gd_5(Si_xGe_{1-x})_4$ alloys is associated with the nature of the first-order phase transition: while the former has a magnetic order-order transition, the latter plays simultaneously a crystallographic order-order phase transition and a magnetic phase transition, the latter being order-disorder for $0.24 \leq x \leq 0.5$ and order-order for $0 \leq x \leq 0.2$ [51, 53, 54, 55]. This magnetoelastic coupling accounts for the rare existence of a first-order magnetic order-disorder phase transition and also for the first-order magnetic order-order phase transition. This is exhaustively developed in Chapter 2.

Following the outburst caused by the discovery of a giant MCE in $Gd_5(Si_xGe_{1-x})_4$ intermetallic alloys, extensive research is being undertaken to find new intermetallic alloys showing first-order field-induced phase transitions, which is generally associated with a strong magnetoelastic coupling. The first obvious step has been to exchange Gd for other rare earth cation in $RE_5(Si_xGe_{1-x})_4$ alloys, with RE=lanthanide [56]. Some of them, such as for example RE=Tb, seem to show magnetoelastic similar properties to that of $Gd_5(Si_xGe_{1-x})_4$, yielding a noticeable MCE (~ -22 J/(kgK) for $\mu_0\Delta H$=5 T at T_t ~110 K) [57]. $Dy_5(Si_xGe_{1-x})_4$ also shows a first-order phase transition for $0.67 \leq x \leq 0.78$, which yields a MCE of ~ -34 J/(kgK) for $\mu_0\Delta H$=5 T at T_t ~65 K [58]. The study of the actual mechanism responsible for the giant MCE in $RE_5(Si_xGe_{1-x})_4$ alloys makes them interesting, but the low temperature transition that show most of these alloys makes them unsuitable from the point of view of applications near room temperature, in contrast to $Gd_5(Si_xGe_{1-x})_4$.

MnAs is also well-known for its first-order magnetoelastic phase transition from FM (with NiAs-type hexagonal crystallographic structure) to PM (with MnP-type orthorhombic structure) order at T_t=318 K, and it might also be a good candidate since it shows giant MCE (-30 J/(kgK) and 13 K for $\mu_0\Delta H$=5 T at T_t). Unfortunately, it is not very useful for applications due to its large thermal hysteresis at the transition [59]. However, the partial substitution of As by Sb in $Mn(As_xSb_{1-x})$ reduces both the thermal hysteresis and the transition temperature, which decreases from 318 K for x=0 to 230 K for x=0.3, maintaining first-order

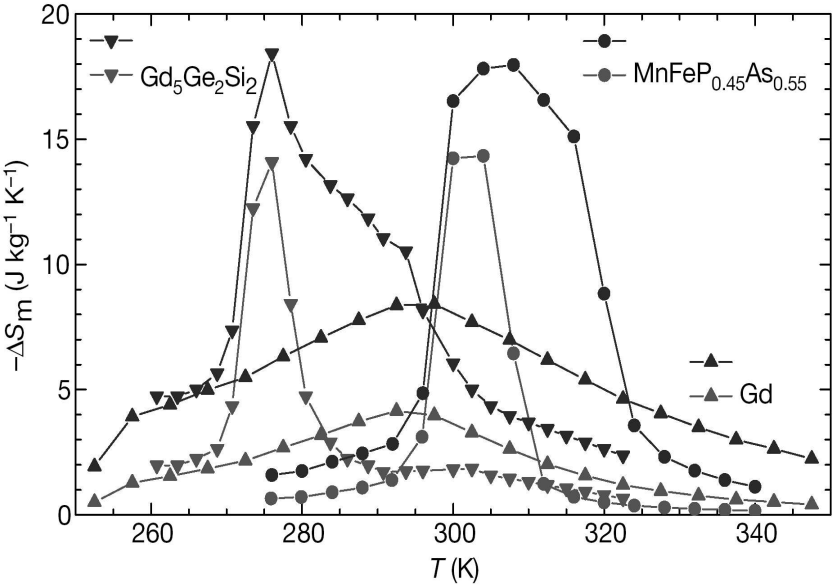

Figure 1.7: Entropy changes of $MnFeP_{0.45}As_{0.55}$ (solid circles), $Gd_5(Si_2Ge_2)$ (inverted solid triangles) and Gd (solid triangles). Data are shown for external field variations of 0-2 T (lower curves for each material), and 0-5 T (upper curves), calculated from magnetisation measurements. Taken from Ref. [63].

and magnetoelastic properties. Hence, a competitive material in a wide temperature range around room temperature is obtained (-25 to -30 J/(kgK) and ~10 K for $\mu_0\Delta H$=5 T) [59, 60]. Moreover, the addition of Fe and P in the $MnFeP_xAs_{1-x}$ alloys still maintains the first-order and field-induced nature of the phase transition near room temperature, for $0.26 \leq x \leq 0.66$ [61, 62]. For example, x=0.45 yields -18 J/(kgK) for $\mu_0\Delta H$=5 T at T_t ~300 K [63]. A comparison of the entropy change of $MnFeP_{0.45}As_{0.55}$ to those of $Gd_5(Si_2Ge_2)$ and pure Gd is given in Fig. 1.7. The advantage in these alloys is that they are transition-metal-based, which are much cheaper than rare earths, and the disadvantage is the poissonousness of the As content [64].

Finally, it has recently been found that the $La(Fe_xSi_{1-x})_{13}$ series of alloys also shows a first-order field-induced FM-PM transition within x=0.86 (T_t ~210 K) and x=0.90 (T_t ~184 K) [65, 66]. However, an itinerant electron metamagnetic transition takes place in this case [66]. That brings about a giant MCE, with an entropy change from -14 to -28 J/(kgK) and a ΔT_{ad} between 6 and 8 K, for $\mu_0\Delta H$=2 T [67, 68, 69]. In order to increase T_t up to room temperature, either Co can be added [70] or hydrogen can be absorbed [68, 69], maintaining the giant effect. Figure 1.8 shows the entropy change and the adiabatic temperature change

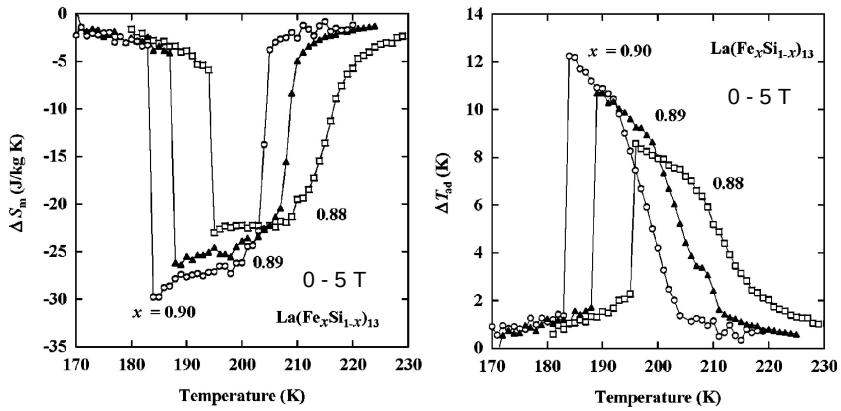

Figure 1.8: Entropy change and adiabatic temperature change for the $La(Fe_xSi_{1-x})_{13}$ compounds with x=0.88, 0.89 and 0.90, when an external field variation 0 to 5 T is provided. Taken from Ref. [69].

obtained for different compositions with a field variation of 0-5 T.

There is another class of materials that also displays a large MCE -the same order than that of Gd-, although not giant. They are the perovskite-like $LaMnO_3$ materials, with Y, Ca, Sr, Li and/or Na substituting for La, and Ti for Mn [71, 72, 73, 74]. The main interest of these compounds is that, showing a MCE similar to that of Gd, they are much cheaper. Their disadvantage with respect to the intermetallic alloys is their low density [75].

A comparision between the above-mentioned materials displaying giant MCE (or MCE similar to that of Gd) is showed in Table 1.1.

1.7 MCE at very low temperature: frustrated magnets and high-spin molecular magnets

At low temperatures, paramagnetic salts are the standard refrigerant materials for magnetic cooling. The higher the density of the magnetic moments and their spin number is, the greater the cooling power of a refrigerant is. With increased density of spins, however, the strength of interactions leads to an ordering transition. The transition temperature thus limits the lowest temperatures achievable with paramagnetic salts. However, in frustrated magnets, the magnetic moments remain disordered and posses finite entropy at temperatures well below the Curie-Weiss constant. For example, large entropy change at low temperature has recently been discovered in $Tb_xY_{1-x}Al_2$ system [2.4 J/(kgK) at T=12 K for a field variation of

Material	T_t (K)	$\mu_0\Delta H$ (T)	ΔS (J/kgK)	ΔT_{ad} (K)	Reference
Gd	294	2/5	-5/-9.8	5.7/11.5	[41, 13]
FeRh	~316	2.1	11.71	-8.4	[50]
$Gd_5(Si_xGe_{1-x})_4$					
$x = 0.5$	276	2/5	-14/-18.5	7.4/15.2	[13]
$x = 0.25$	~136	5	-68	12	[38, 39]
$Tb_5(Si_xGe_{1-x})_4$					
$x = 0.5$	~110	5	-21.8	-	[57]
$Dy_5(Si_xGe_{1-x})_4$					
$x = 0.75$	~65	5	-34	-	[58]
$La(Fe_xSi_{1-x})_{13}$					
$x = 0.877$	208	2/5	-14.3/-19.4	-	[67]
$x = 0.880$	195	2/5	-20/-23	6.5/8.6	[68, 69]
$x = 0.890$	188	2/5	-24/-26	7.5/10.7	[68, 69]
$x = 0.900$	184	2/5	-28/-30	8.1/12.1	[68, 69]
$La(Fe_{0.88}Si_{0.12})_{13}H_{1.0}$	274	2	-19/-23	6.2/11.1	[68, 69]
$La(Fe_{0.89}Si_{0.11})_{13}H_{1.3}$	291	2	-24/-28	6.9/12.8	[68, 69]
$La(Fe_{11.2}Co_{0.7}Si_{1.1})$	274	2/5	-12/-20.3	-	[70]
MnAs-based					
$Mn(As_xSb_{1-x})$					
$x = 1$	318	2/5	-31/-32	4.7/13	[59]
$x = 0.1$	283	2/5	-24/-30	-	[59]
$x = 0.25$	230	2/5	-18/-23	5.5/10	[60]
$MnFeP_{0.45}As_{0.55}$	~300	2/5	-14.5/-18	-	[63]
Ceramic manganites					
$La_{0.8}Ca_{0.2}MnO_3$	230	1.5	-5.5	<2.5	[72, 75]
$La_{0.6}Ca_{0.4}MnO_3$	263	3	-5.0	<2.4	[73, 75]
$La_{0.84}Sr_{0.16}MnO_3$	243.5	2.5/5/8	-3.8/-5.5/-7.9	-/-/<4.1	[74, 75]

Table 1.1: Entropy change, ΔS, and adiabatic temperature change, ΔT_{ad}, ocurring at the transition temperature T_t, at different values of applied field increase, ΔH, for materials displaying giant magnetocaloric effect. The prototype material at room temperature, Gd, is also showed for comparision.

$\mu_0\Delta H$=2 T and 7.6 J/(kgK) at T=30 K for $\mu_0\Delta H$=2 T], associated with the spin-glass-to-PM (freezing) transition [76]. Moreover, enhanced magnetocaloric effect has been predicted in geometrically frustrated magnets [77]. This enhancement is related to the presence of a macroscopic number of soft modes associated with geometrical frustration below the saturation field.

Another interesting type of materials showing large (and time-dependent) entropy change at very low temperature are the high-spin molecular magnets. Molecular clusters as Mn_{12} and Fe_8 exhibit extremely high entropy change around the blocking temperature at the Kelvin regime, which is associated with the order-disorder blocking process. Values of 21 J/(kgK) at $T \simeq 3$ K for a field variation of $\mu_0\Delta H$=3 T at a sweeping rate of 0.01 Hz are obtained for Mn_{12} [78]. Therefore, they are potential candidates to magnetic refrigerants in the helium liquefaction regime.

1.8 Magnetic refrigeration

Currently, there is a great deal of interest in utilizing the MCE as an alternate technology for refrigeration both in the ambient temperature and in cryogenic temperatures. Magnetic refrigeration is an environmentally friendly cooling technology (see Fig. 1.9 for details). It does not use ozone-depleting chemicals (such as chlorofluorocarbons), hazardous chemicals (such as ammonia), or greenhouse gases (hydrochlorofluorocarbons and hydrofluorocarbons). Most modern refrigeration systems and air conditioners still use ozone-depleting or global-warming volatile liquid refrigerants. Magnetic refrigerators use a solid refrigerant (usually in a form of spheres or thin sheets) and common heat transfer fluids (e.g. water, water-alcohol solution, air, or helium gas) with no ozone-depleting and/or global-warming effects. Another important difference between vapour-cycle refrigerators and magnetic refrigerators is the amount of energy loss incurred during the refrigeration cycle. Even the newest most efficient commercial refrigeration units operate well below the maximum theoretical (Carnot) efficiency, and few, if any, further improvements may be possible with the existing vapor-cycle technology. Magnetic refrigeration, however, is rapidly becoming competitive with conventional gas compression technology because it offers considerable operating cost savings by eliminating the most inefficient part of the refrigerator: the compressor. The cooling efficiency of magnetic refrigerators working with Gd has been shown [2, 6, 7, 79] to reach 60% of the Carnot limit, compared to only about 40% in the best gas-compression refrigerators. However, with the currently available magnetic materials, this high efficiency is only realised in high magnetic fields of 5 T. Therefore, research for new magnetic materials displaying larger MCE, which then can be operated in lower fields of about 2 T that can be generated by

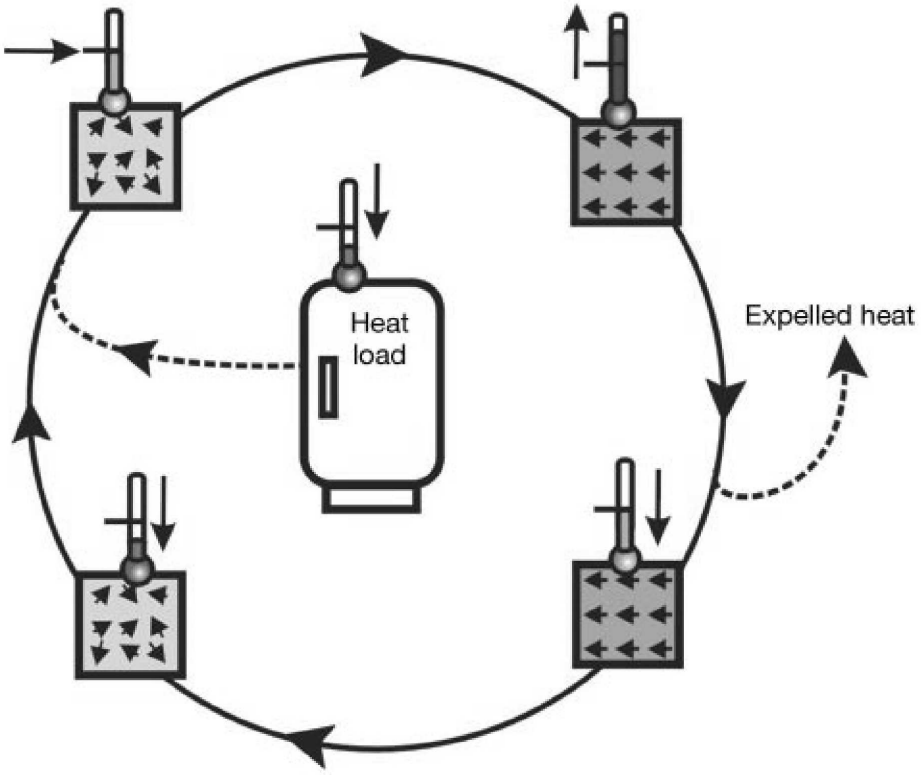

Figure 1.9: Schematic representation of a magnetic-refrigeration cycle, which transports heat from the heat load to its surroundings. Light and dark grey depict the magnetic material without and with applied magnetic field, respectively. Initially disordered magnetic moments are aligned by a magnetic field, resulting in heating of the magnetic material. This heat is removed from the material to its surroundings by a heat-transfer medium. On removing the field, the magnetic moments randomize, which leads to cooling of the magnetic material below the ambient temperature. Heat from the system to be cooled can then be extracted using a heat-transfer medium. Taken from Ref. [63].

permanent magnets, is very significant. The heating and cooling that occurs in the magnetic refrigeration technique is proportional to the size of the magnetic moments and to the applied magnetic field. This is why research in magnetic refrigeration is at present almost exclusively conducted on superparamagnetic materials and on rare-earth compounds.

Refrigeration in the subroom temperature (~250-290 K) range is of particular interest because of potential impact on energy savings and environmental concerns. As described along this chapter, materials to be applied in magnetic refrigeration must present a series of properties:

(i) A first-order field-induced transition around the working temperature, in order to utilise the associated entropy change.

(ii) A high refrigerant capacity. Refrigerant capacity, q, is a measure of how much heat can be transferred between the cold and hot sinks in one ideal refrigeration cycle, and it is calculated as:

$$q = \int_{T_{\mathrm{cold}}}^{T_{\mathrm{hot}}} \Delta S(T)_{\Delta H}\, dT \quad . \tag{1.18}$$

Therefore, a large entropy change in a temperature range as wide as possible is needed. Moreover, it is easy to argue that for any practical application it is the amount of heat energy per unit volume transferred in one refrigeration cycle, which is the important parameter, *i.e.*, the denser the magnetic refrigerant the more effective it is [75].

(iii) A low magnetic hysteresis, to avoid magnetic-work losses due to the rotation of domains in a magnetic-refrigeration cycle.

(iv) A low heat capacity C_P, since a high C_P increases the thermal load and more energy is required to heat the sample itself and causes a loss in entropy, *i.e.* for a given ΔS, ΔT_{ad} will be lower.

(v) Low cost and harmless. The main problem of the rare-earth-based compounds, which are usually the best magnetic refrigerants in the whole temperature range (including pure Gd at room temperature) is their high cost. 3*d*-transition-metal compounds or ceramic manganites are a good alternative concerning the cost of the materials. In particular, the recently reported MnAs-based materials show good prospects [59, 63]. However, the presence of As in these compounds, which is poisonous, could make them be useless for commercial applications. Another type of compounds, $La(Fe_xSi_{1-x})_{13}$, also presents a large MCE at room temperature, has a low cost and in this case all elements are harmless [68, 69].

Bibliography

[1] A. M. Tishin, in *Handbook of Magnetic Materials*, edited by K. H. J. Buschow (North Holland, Amsterdam, 1999), Vol. 12, pp. 395–524.

[2] V. K. Pecharsky and K. A. Gschneidner, Jr., J. Magn. Magn. Mater.**200**, 44 (1999).

[3] E. Warburg, Ann. Phys. **13**, 141 (1881).

[4] P. Debye, Ann. Phys. **81**, 1154 (1926).

[5] W. F. Giauque, J. Amer. Chem. Soc. **49**, 1864 (1927).

[6] V. K. Pecharsky and K. A. Gschneidner, Jr., J. Appl. Phys.**85**, 5365 (1999).

[7] K. A. Gschneidner, Jr. and V. K. Pecharsky, Annu. Rev. Mater. Sci.**30**, 387 (2000).

[8] A. H. Morrish, *The Physical Principles of Magnetism* (Wiley, New York, 1965), Chap. 3.

[9] A. M. Tishin, K. A. Gschneidner, Jr., and V. K. Pecharsky, Phys. Rev. B**59**, 503 (1999).

[10] S. Y. Dan'kov, A. M. Tishin, V. K. Pecharsky, and K. A. Gschneidner, Jr., Rev. Sci. Instrum. **68**, 2432 (1997).

[11] B. R. Gopal, R. Chahine, and T. K. Bose, Rev. Sci. Instrum.**68**, 1818 (1997).

[12] M. Földeàki, R. Chahine, and T. K. Bose, J. Appl. Phys.**77**, 3528 (1995).

[13] V. K. Pecharsky and K. A. Gschneidner, Jr., Phys. Rev. Lett.**78**, 4494 (1997).

[14] M. W. Zemansky, *Heat and Thermodynamics*, 6th ed. (McGraw-Hill, New York, 1981).

[15] V. K. Pecharsky and K. A. Gschneidner, Jr., Adv. Cryog. Eng. **42A**, 423 (1996).

[16] V. K. Pecharsky and K. A. Gschneidner, Jr., J. Appl. Phys.**86**, 6315 (1999).

[17] V. K. Pecharsky, K. A. Gschneidner, Jr., A. O. Pecharsky, and A. M. Tishin, Phys. Rev. B **64**, 144406 (2001).

[18] W. F. Giauque and I. P. D. McDougall, Phys. Rev.**43**, 768 (1933).

[19] A. H. Cooke, Proc. Roy. Soc. A **62**, 269 (1949).

[20] B. Bleaney, Proc. Roy. Soc. A **204**, 203 (1950).

[21] A. H. Cooke, H. J. Duffus, and W. P. Wolf, Philos. Mag. **44**, 623 (1953).

[22] H. Ishimoto, N. Nishida, T. Furubayashi, M. Shinohara, Y. Takano, Y. Miura, and K. Ono, J. Low Temp. Phys. **55**, 17 (1984).

[23] A. E. Clark and R. S. Alben, J. Appl. Phys. **41**, 1195 (1970).

[24] V. Nekvasil, V. Roskovec, F. Zounova, and P. Novotny, Czech. J. Phys. **24**, 810 (1974).

[25] R. Z. Levitin, V. V. Snegirev, A. V. Kopylov, A. S. Lagutin, and A. Gerber, J. Magn. Magn. Mat. **170**, 223 (1997).

[26] R. D. Shull, R. D. McMichael, and J. J. Ritter, Nanostruct. Mater. **2**, 205 (1993).

[27] C. B. Zimm, P. M. Ratzmann, J. A. Barclay, G. F. Green, and J. N. Chafe, Adv. Cryog. Eng. **36**, 763 (1990).

[28] C. B. Zimm, P. L. Kral, J. A. Barclay, G. F. Green, and W. G. Patton, in *Proceedings of the 5th International Cryocooler Conference* (Wright Research and Development Center, Wright Patterson Air Force base, Ohio, 1988), p. 49.

[29] C. B. Zimm, J. A. Barclay, H. H. Harkness, G. F. Green, and W. G. Patton, Cryogenics **29**, 937 (1989).

[30] T. Hashimoto, T. Kuzuhara, M. Sahashi, K. Inomata, A. Tomokiyo, and H. Yayama, J. Appl. Phys. **62**, 3873 (1987).

[31] H. Takeya, V. K. Pecharsky, K. A. Gschneidner, Jr., and J. O. Moorman, Appl. Phys. Lett. **64**, 2739 (1994).

[32] J. A. Barclay, W. C. Overton, and C. B. Zimm, in *LT-17 Contributed Papers*, edited by U. Ekren, A. Schmid, W. Weber, and H. Wuhl (Elsevier Science, Amsterdam, 1984), p. 157.

[33] C. B. Zimm, E. M. Ludeman, M. C. Serverson, and T. A. Henning, Adv. Cryog. Eng. **37B**, 883 (1992).

[34] A. Tomokiyo, H. Yayama, H. Wakabayashi, T. Kuzuhara, T. Hashimoto, M. Sahashi, and K. Inomata, Adv. Cryog. Eng. **32**, 295 (1986).

[35] S. M. Benford, J. Appl. Phys. **50**, 1868 (1979).

[36] X. Y. Liu, J. A. Barclay, M. Földeàki, B. R. Gopal, R. Chahine, and T. K. Bose, Adv. Cryog. Eng. **42A**, 431 (1997).

[37] M. Földeàki, R. Chahine, B. R. Gopal, T. K. Bose, X. Y. Liu, and J. A. Barclay, J. Appl. Phys. **83**, 2727 (1998).

[38] V. K. Pecharsky and K. A. Gschneidner, Jr., Appl. Phys. Lett. **70**, 3299 (1997).

[39] V. K. Pecharsky and K. A. Gschneidner, Jr., Adv. Cryog. Eng. **43**, 1729 (1998).

[40] S. M. Benford and G. Brown, J. Appl. Phys. **52**, 2110 (1981).

[41] S. Y. Dan'kov, A. M. Tishin, V. K. Pecharsky, and K. A. Gschneidner, Jr., Phys. Rev. B **57**, 3478 (1998).

[42] S. A. Nikitin, A. S. Andreenko, A. M. Tishin, A. M. Arkharov, and A. A. Zherdev, Fiz. Met. Metalloved. **56**, 327 (1985).

[43] A. Smaili and R. Chahine, J. Appl. Phys. **81**, 824 (1997).

[44] M. Földeàki, W. Schnelle, E. Gmelin, P. Benard, B. Koszegui, A. Giguère, R. Chahine, and T. K. Bose, J. Appl. Phys. **82**, 309 (1997).

[45] Y. Z. Shao, J. K. L. Lai, and C. H. Shek, J. Magn. Magn. Mater. **163**, 103 (1996).

[46] S. Y. Dan'kov, V. V. Ivtchenko, A. M. Tishin, K. A. Gschneidner, Jr., and V. K. Pecharsky, Adv. Cryog. Eng. **46A**, 397 (2000).

[47] S. Jin, L. Liu, Y. Wang, and B. Chen, J. Appl. Phys. **70**, 6275 (1991).

[48] A. J. P. Meyer and P. Tanglang, J. Phys. Rad. **14**, 82 (1953).

[49] A. Giguère, M. Földeàki, B. Ravi Gopal, R. Chahine, T. K. Bose, A. Frydman, and J. A. Barclay, Phys. Rev. Lett. **83**, 2262 (1999).

[50] M. P. Annaorazov, S. A. Nikitin, A. L. Tyurin, K. A. Asatryan, and A. K. Dovletov, J. Appl. Phys. **79**, 1689 (1996).

[51] V. K. Pecharsky and K. A. Gschneidner, Jr., J. Alloys Comp. **260**, 98 (1997).

[52] V. K. Pecharsky and K. A. Gschneidner, Jr., J. Magn. Magn. Mater. **167**, L179 (1997).

[53] L. Morellon, P. A. Algarabel, M. R. Ibarra, J. Blasco, B. García-Landa, Z. Arnold, and F. Albertini, Phys. Rev. B **58**, R14721 (1998).

[54] L. Morellon, J. Blasco, P. A. Algarabel, and M. R. Ibarra, Phys. Rev. B **62**, 1022 (2000).

[55] V. K. Pecharsky and K. A. Gschneidner, Jr., Adv. Mater. **13**, 683 (2001).

[56] K. A. Gschneidner, Jr., V. K. Pecharsky, A. O. Pecharsky, V. V. Ivtchenko, and E. M. Levin, J. Alloys Comp. **303-304**, 214 (2000).

[57] L. Morellon, C. Magen, P. A. Algarabel, M. R. Ibarra, and C. Ritter, Appl. Phys. Lett. **79**, 1318 (2001).

[58] V. V. Ivtchenko, V. K. Pecharsky, and K. A. Gschneidner, Jr., Adv. Cryog. Eng. **46A**, 405 (2000).

[59] H. Wada and Y. Tanabe, Appl. Phys. Lett. **79**, 3302 (2001).

[60] H. Wada, T. Morikawa, K. Taniguchi, T. Shibata, Y. Yamada, and Y. Akishige, Physica B **328**, 114 (2003).

[61] R. Zach, M. Guillot, and R. Fruchart, J. Magn. Magn. Mater. **89**, 221 (1990).

[62] M. Bacmann, J. L. Soubeyroux, R. Barrett, D. Fruchart, R. Zach, S. Niziol, and R. Fruchart, J. Magn. Magn. Mater. **134**, 59 (1994).

[63] O. Tegus, E. Brück, K. H. J. Buschow, and F. R. de Boer, Nature **415**, 450 (2002).

[64] For an interesting debate, see for example "El País", March 6th, 2002.

[65] A. Fujita, Y. Akamatsu, and K. Fukamichi, J. Appl. Phys. **85**, 4756 (1999).

[66] A. Fujita, S. Fujieda, K. Fukamichi, H. Mitamura, and T. Goto, Phys. Rev. B **65**, 14410 (2001).

[67] F. X. Hu, B. G. Shen, J. R. Sun, Z. H. Cheng, G. H. Rao, and X. X. Zhang, Appl. Phys. Lett. **78**, 3675 (2001).

[68] S. Fujieda, A. Fujita, and K. Fukamichi, Appl. Phys. Lett. **81**, 1276 (2002).

[69] A. Fujita, S. Fujieda, Y. Hasegawa, and K. Fukamichi, Phys. Rev. B **67**, 104416 (2003).

[70] F. X. Hu, B. G. Shen, J. R. Sun, G. J. Wang, and Z. H. Cheng, Appl. Phys. Lett. **80**, 826 (2002).

[71] X. X. Zhang, J. Tejada, Y. Xin, G. F. Sun, K. W. Wong, and X. Bohigas, Appl. Phys. Lett. **69**, 3596 (1996).

[72] Z. B. Guo, Y. W. Du, J. S. Zhu, H. Huang, W. P. Ding, and D. Feng, Phys. Rev. Lett. **78**, 1142 (1997).

[73] X. Bohigas, J. Tejada, E. del Barco, X. X. Zhang, and M. Sales, Appl. Phys. Lett. **73**, 390 (1998).

[74] A. Szewczyk, H. Szymczak, A. Wisniewski, K. Piotrowski, R. Kartaszyński, B. Dabrowski, S. Koleśnik, and Z. Bukowski, Appl. Phys. Lett. **77**, 1026 (2000).

[75] V. K. Pecharsky and K. A. Gschneidner, Jr., J. Appl. Phys.**90**, 4614 (2001).

[76] X. Bohigas, J. Tejada, F. Torres, J. I. Arnaudas, E. Joven, and A. del Moral, Appl. Phys. Lett. **81**, 2427 (2002).

[77] M. E. Zhitomirsky, Phys. Rev. B **67**, 104421 (2003).

[78] F. Torres, J. M. Hernández, X. Bohigas, and J. Tejada, Appl. Phys. Lett.**77**, 3248 (2000).

[79] C. B. Zimm, A. Jastrab, A. Sternberg, V. K. Pecharsky, K. A. Gschneidner, Jr., M. Osborne, and I. Anderson, Adv. Cryog. Eng.**43**, 1759 (1998).